Coupling impedance of beam pipes of general cross section

Robert L. Gluckstern and Johannes van Zeijts

Physics Department, University of Maryland, College Park, Maryland 20742

Bruno Zotter

SL Division, CERN, Geneva 23, Switzerland

(Received 24 June 1992)

We have derived expressions for the longitudinal and transverse resistive wall coupling impedances for a beam pipe of arbitrary cross section in the ultrarelativistic limit. These expressions involve the integral of the square of the tangential magnetic fields along the wall, which can be obtained from the solution of the two-dimensional Poisson equations with a monopole and dipole singularity, respectively. Explicit results are given for beam pipes of elliptical and rectangular cross sections, including the limiting cases of a circle and a pair of parallel plates.

PACS number(s): 41.75.−i

I. INTRODUCTION

We have recently calculated the longitudinal and transverse resistive wall coupling impedances in a beam pipe of elliptical cross section for an ultrarelativistic beam [1]. Since the general features of the calculation are independent of the beam pipe cross section at ultrarelativistic velocities, we extend it here and include the results for elliptic and rectangular beam pipes.

In Sec. II, we derive an expression for the longitudinal coupling impedance as an integral over a Poynting-like vector at the surface of the beam pipe generated by an ultrarelativistic beam along the axis of the beam pipe. The same technique is applied in Sec. III to the transverse coupling impedance, but for fields generated by a line dipole beam along the axis of the beam pipe, obtained by a simple limiting process involving a beam off axis. In Sec. IV we obtain the necessary fields for an elliptical beam pipe and in Sec. V for a rectangular beam pipe. In these sections we also derive the image fields from which the parameters appropriate to the coherent and incoherent tune shifts can be obtained. Finally in Sec. VI we present the results for the coupling impedances, including numerical results for different ellipticities and aspect ratios.

II. LONGITUDINAL COUPLING IMPEDANCE

For a drive beam of current density

$$J_z = I_0 \delta(x - x_1)\delta(y - y_1)\exp(-jkz) \qquad (2.1)$$

in the frequency domain, with $k = \omega/c$, the longitudinal impedance is defined as

$$Z_{\parallel}(k) = -\frac{1}{I_0}\int_{-\infty}^{\infty} dz\, E_z e^{jkz}, \qquad (2.2)$$

where E_z is the longitudinal component of the electric field when $x_1 = 0, y_1 = 0$. We use Eq. (2.1) to rewrite $Z_{\parallel}(k)$ as

$$Z_{\parallel}(k) = -\frac{1}{|I_0|^2}\int dv\, \mathbf{E}\cdot\mathbf{J}^*, \qquad (2.3)$$

where the volume integral is over a region which includes the drive beam.

We now consider two situations. The first, denoted by the subscript 1, is the lossless pipe, and the second, denoted by the subscript 2, is the pipe with wall losses. We then construct

$$|I_0|^2[Z_{\parallel}^{(2)}(k) + Z_{\parallel}^{(1)*}(k)] = |I_0|^2[Z_{\parallel}^{(2)}(k) - Z_{\parallel}^{(1)}(k)]$$
$$= -\int dv[\mathbf{E}_2\cdot\mathbf{J}^* + \mathbf{E}_1^*\cdot\mathbf{J}], \qquad (2.4)$$

where $Z_{\parallel}^{(1)}(k)$ is imaginary. (It actually vanishes in the ultrarelativistic limit.) Using

$$\mathbf{J} = \nabla\times\mathbf{H}_{1,2} - j\omega\epsilon\mathbf{E}_{1,2},$$
$$\nabla\times\mathbf{E}_{1,2} = -j\omega\mu\mathbf{H}_{1,2}, \qquad (2.5)$$

Eq. (2.4) can be converted into a surface integral, leading to

$$|I_0|^2 Z_{\parallel}(k) = \int dS\, \mathbf{n}\cdot[\mathbf{E}_2\times\mathbf{H}_1^* + \mathbf{E}_1^*\times\mathbf{H}_2], \qquad (2.6)$$

where the surface encloses the drive beam. If we choose S to be the inside surface of the beam pipe, $\mathbf{n}\cdot\mathbf{E}_1^*\times\mathbf{H}_2 = 0$, and we have, for a length of beam pipe L,

$$|I_0|^2 Z_{\parallel}(k) = -L\oint ds E_z H_{1s}^*, \qquad (2.7)$$

where s is a coordinate tangential to the beam pipe surface in a plane perpendicular to the axis of the beam pipe. The form in Eq. (2.7) is a generalization of a result derived earlier [2] for a beam pipe of circular cross section and used recently by Napoly [3].

We now obtain the result for a resistive wall by expressing E_z at the wall in terms of H_{1s}. Specifically we take

$$E_z \cong -k\delta(1 + j)Z_0 H_{1s}/2, \qquad (2.8)$$

where $\delta = (2/k\sigma Z_0)^{1/2}$ is the skin depth of the wall material whose conductivity is σ. Here $Z_0 = (\mu/\epsilon)^{1/2} \cong 120\pi$ Ω is the impedance of free space. Using Eq. (2.8), we write the longitudinal impedance as

$$|I_0|^2 Z_{\parallel}(k)/Z_0 = (1+j)(kL\delta/2) \oint ds |H_{1s}|^2. \qquad (2.9)$$

Finally, H_{1s} can be obtained from the solution of the Laplace (or Poisson) equation in the two transverse dimensions since $c^2 \partial^2/\partial z^2 = \partial^2/\partial t^2$ for an ultrarelativistic particle. Specifically

$$Z_0 H_{1s} = E_{1n} = -\exp(-jkz)\nabla_{\perp}\Phi(x,y), \qquad (2.10)$$

where $\Phi(x,y)$ is the solution of

$$\nabla_{\perp}^2 \Phi(x,y) = -Z_0 I_0 \delta(x-x_1)\delta(y-y_1), \qquad (2.11)$$

with perfectly conducting boundary conditions at the beam pipe wall. Here n is a coordinate normal to the beam pipe wall and E_{1n} is the electric field normal to the beam pipe surface for the lossless problem.

III. TRANSVERSE COUPLING IMPEDANCE

The transverse coupling impedance can be analyzed in a similar manner. If we start with the axial dipole drive current

$$J_z = I_0 \delta(y)\exp(-jkz)[\delta(x-x_1) - \delta(x+x_1)], \qquad (3.1)$$

the transverse impedance in the x direction can be expressed as the limit for small x_1 of

$$Z_x(k) = -\frac{1}{2kI_0 x_1} \int_{-\infty}^{\infty} dz \frac{\partial E_z}{\partial x} e^{jkz}, \qquad (3.2)$$

where $\partial E_z/\partial x$ is evaluated for $x = y = 0$. But we can also write the derivative of E_z at the origin as

$$\frac{\partial E_z}{\partial x} = \frac{E_z(x_1,0,z) - E_z(-x_1,0,z)}{2x_1} \qquad (3.3)$$

for vanishingly small x_1. Thus we have

$$Z_x(k) = -\frac{1}{4kI_0 x_1^2} \int_{-\infty}^{\infty} dz[\, E_z(x_1,0,z)$$
$$-E_z(-x_1,0,z)]e^{jkz}. $$

Using the value of $\mathbf{J}$ in Eq. (3.1), we can therefore write

$$Z_x(k) = -\frac{1}{4kx_1^2|I_0|^2} \int dv \mathbf{E} \cdot \mathbf{J}^*, \qquad (3.4)$$

in analogy with Eq. (2.3). As before, the volume integral in Eq. (3.5) can be written as a surface integral, and we obtain

$$4x_1^2 |I_0|^2 kZ_x(k) = -L \oint ds E_z H_{1s}^*, \qquad (3.5)$$

where we must now use the fields corresponding to the dipole configuration in Eq. (3.1). Finally, we use Eq. (2.8) to obtain

$$4x_1^2 |I_0|^2 Z_x(k)/Z_0 = (1+j)(L\delta/2) \oint ds |H_{1s}|^2. \qquad (3.6)$$

IV. BEAM PIPE OF ELLIPTICAL CROSS SECTION

A. Elliptic coordinates

The Poisson equation for the electrostatic potential of a line charge of density λ located at $x = x_1, y = y_1$ is

$$\frac{\partial^2 \Phi}{\partial x^2} + \frac{\partial^2 \Phi}{\partial y^2} = -\frac{\lambda}{\epsilon_0}\delta(x-x_1)\delta(y-y_1), \qquad (4.1)$$

where λ/ϵ_0 can be written in terms of the drive current as $\lambda/\epsilon_0 = Z_0 I_0$. We transform to elliptic coordinates defined by

$$x = c\cosh u \cos v, \qquad (4.2)$$

$$y = c\sinh u \sin v, \qquad (4.3)$$

where the beam pipe is an ellipse of major axis $2a$, minor axis $2b$, with

$$a = c\cosh u_0 \ , \ b = c\sinh u_0 \ , \ c^2 = a^2 - b^2. \qquad (4.4)$$

In the transformed coordinate system, Eq. (4.1) becomes

$$\frac{\partial^2 \Phi}{\partial u^2} + \frac{\partial^2 \Phi}{\partial v^2} = -Z_0 I_0 \delta(u-u_1)\delta(v-v_1), \qquad (4.5)$$

where u_1, v_1 are related to x_1, y_1 by Eqs. (4.2) and (4.3). We write the solution to Eq. (4.5) as

$$\Phi(u,v) = f_0(u) + \sum_{n=1}^{\infty} f_n(u)\cos nv + \sum_{n=1}^{\infty} g_n(u)\sin nv, \qquad (4.6)$$

where $f_n(u)$ and $g_n(u)$ are some linear combination of $\exp(\pm nu)$.

Substituting Eq. (4.6) into Eq. (4.5) and expanding $\delta(v-v_1)$, we obtain

$$\frac{d^2 f_0}{du^2} = -\frac{Z_0 I_0}{2\pi}\delta(u-u_1), \qquad (4.7)$$

$$\frac{d^2 f_n}{du^2} - n^2 f_n = -\frac{Z_0 I_0}{\pi}\delta(u-u_1)\cos nv_1, \qquad (4.8)$$

$$\frac{d^2 g_n}{du^2} - n^2 g_n = -\frac{Z_0 I_0}{\pi}\delta(u-u_1)\sin nv_1. \qquad (4.9)$$

We seek solutions to Eq. (4.1) which are well behaved at $x = 0, y = 0$. Since

$$x + iy = c\cosh(u+iv), \qquad (4.10)$$

well-behaved solutions correspond to the form $\cosh n(u+iv)$. Since

$$\cosh nw = T_n(\cosh w), \qquad (4.11)$$

where T_n is the nth Tschebyscheff polynomial, the function

$$\cosh n(u + iv) = T_n\left(\frac{x + iy}{c}\right) \qquad (4.12)$$

is regular at $x = 0, y = 0$ and its real and imaginary parts guide us to the forms

$$f_n(u) = \cosh nu \ , \ g_n(u) = \sinh nu. \qquad (4.13)$$

$$f_0(u) = \frac{Z_0 I_0}{2\pi}\begin{cases} u_0 - u_1 \ , & 0 \le u \le u_1 \\ u_0 - u \ , & u_1 \le u \le u_0 \end{cases} \qquad (4.14)$$

$$f_n(u) = \frac{Z_0 I_0 \cos nv_1}{\pi \cosh nu_0}\begin{cases} \cosh nu \sinh n(u_0 - u_1) \ , & 0 \le u \le u_1 \\ \sinh n(u_0 - u)\cosh nu_1 \ , & u_1 \le u \le u_0 \end{cases} , \quad n \ge 1, \qquad (4.15)$$

$$g_n(u) = \frac{Z_0 I_0 \sin nv_1}{\pi \sinh nu_0}\begin{cases} \sinh nu \sinh n(u_0 - u_1) \ , & 0 \le u \le u_1 \\ \sinh n(u_0 - u)\sinh nu_1 \ , & u_1 \le u \le u_0 \end{cases} , \quad n \ge 1. \qquad (4.16)$$

The term proportional to u_0 in Eq. (4.14) is a constant which will not enter into the fields. It will therefore be omitted.

Use of Eqs. (4.14)–(4.16) in Eq. (4.6) yields the two-dimensional Green function in an elliptical pipe [4]. From this, we obtain for the component of the electric field normal to the elliptical boundary

$$E_u = -\frac{1}{h}\frac{\partial \Phi}{\partial u} = \frac{Z_0 I_0}{2\pi}\frac{Q(v)}{h(v)}. \qquad (4.17)$$

Here

$$Q(v) = 1 + 2\sum_{n=1}^{\infty}\frac{\cosh nu_1 \cos nv_1 \cos nv}{\cosh nu_0}$$
$$+ 2\sum_{n=1}^{\infty}\frac{\sinh nu_1 \sin nv_1 \sin nv}{\sinh nu_0} \qquad (4.18)$$

and $h(v)$ is the metric

$$h(v) = c(\sinh^2 u_0 + \sin^2 v)^{1/2} \qquad (4.19)$$

at the elliptical boundary. For later use, we expand $Q(v)$ up to linear terms in x_1 and y_1. For this purpose we write

$$\cosh nu_1 \cos nv_1 + i \sinh nu_1 \sin nv_1$$

$$= \cosh n(u_1 + iv_1)$$

$$= T_n\left(\frac{x_1 + iy_1}{c}\right)$$

$$= \cos\frac{n\pi}{2} + n\sin\frac{n\pi}{2}\left(\frac{x_1 + iy_1}{c}\right) + \cdots \qquad (4.20)$$

and find

$$Q(v) = Q_0(v) + \frac{x_1}{c}Q_{1x}(v) + \frac{y_1}{c}Q_{1y}(v) + \cdots \qquad (4.21)$$

with

$$Q_0(v) = 1 + 2\sum_{m=1}^{\infty}(-1)^m\frac{\cos 2mv}{\cosh 2mu_0}, \qquad (4.22)$$

B. Green functions

We now construct the one-dimensional Green-function solutions to Eqs. (4.7), and find for the functions which vanish at the elliptical boundary, $u = u_0$,

$$Q_{1x}(v) = 2\sum_{m=0}^{\infty}(-1)^m(2m+1)\frac{\cos(2m+1)v}{\cosh(2m+1)u_0}, \qquad (4.23)$$

$$Q_{1y}(v) = 2\sum_{m=0}^{\infty}(-1)^m(2m+1)\frac{\sin(2m+1)v}{\sinh(2m+1)u_0}. \qquad (4.24)$$

These infinite sums can also be expressed in closed form in terms of the Jacobi elliptic functions sn, cn, and dn of argument $\overline{v} = 2Kv/\pi$, where $K(k)$ is the complete elliptic integral of modulus k corresponding to the "nome" $q = \exp(-2u_0) = |a - b|/(a + b)$. From the Fourier expansions for these functions [5] one finds readily

$$Q_0(v) = \left(\frac{2K}{\pi}\right)\frac{k'}{\mathrm{dn}(\overline{v}, q)}, \qquad (4.25)$$

$$Q_{1x}(v) = \left(\frac{2K}{\pi}\right)^2 kk'\frac{\mathrm{cn}(\overline{v}, q)}{\mathrm{dn}^2(\overline{v}, q)}, \qquad (4.26)$$

$$Q_{1y}(v) = \left(\frac{2K}{\pi}\right)^2 kk'^2\frac{\mathrm{sn}(\overline{v}, q)}{\mathrm{dn}^2(\overline{v}, q)}, \qquad (4.27)$$

which have been verified by computer for the range $0 < u_0 < 1$ and $0 < v < \pi/2$. Similar expressions for an elliptical beam pipe have also been given by Palumbo and Vaccaro [6].

C. Image potential

Although it is not needed for the coupling impedance, we also derive the potential due to the images alone since the results involve many of the same combinations of parameters as for the impedance. This image potential can be used to calculate the coherent and incoherent tune shifts due to the beam which may be important in avoiding resonances.

The image potential can be found by obtaining $f_n(u), g_n(u)$ when the boundary is infinitely far away and subtracting these values from Eqs. (4.14)–(4.16). Specifically, the limit $u_0 \to \infty$ leads to the coefficients for the

"self" potentials

$$f_0^{(s)}(u) = \frac{Z_0 I_0}{\pi} \begin{cases} -u_1 \ , & 0 \le u \le u_1 \\ -u \ , & u_1 \le u, \end{cases} \tag{4.28}$$

$$f_n^{(s)}(u) = \frac{Z_0 I_0 \cos nu_1}{\pi} \begin{cases} e^{-nu_1} \cosh nu \ , & 0 \le u \le u_1 \\ e^{-nu} \cosh nu_1 \ , & u_1 \le u \end{cases} \tag{4.29}$$

$$g_n^{(s)}(u) = \frac{Z_0 I_0 \sin nu_1}{\pi} \begin{cases} e^{-nu_1} \sinh nu \ , & 0 \le u \le u_1 \\ e^{-nu} \sinh nu_1 \ , & u_1 \le u \end{cases} \tag{4.30}$$

and to the coefficients for the image potentials

$$f_n^{(i)}(u) = f_n(u) - f_n^{(s)}(u), \tag{4.31}$$

$$g_n^{(i)}(u) = g_n(u) - g_n^{(s)}(u)$$

given by

$$f_0^{(i)}(u) = 0, \tag{4.32}$$

$$f_n^{(i)}(u) = -\frac{Z_0 I_0 e^{-nu_0}}{\pi \cosh nu_0} \cosh nu \cosh nu_1 \cos nv_1, \tag{4.33}$$

$$g_n^{(i)}(u) = -\frac{Z_0 I_0 e^{-nu_0}}{\pi \sinh nu_0} \sinh nu \sinh nu_1 \sin nv_1, \tag{4.34}$$

where Eqs. (4.29), (4.30), and (4.33), (4.34) apply for $n \ge 1$. The image potential, obtained by using Eqs. (4.33) and (4.34) in Eq. (4.6), correctly vanishes as $u_0 \to \infty$, and has no discontinuous derivative at $u = u_1$. Such a discontinuity is present only in the self-field.

Using Eqs. (4.32)–(4.34), we find for the image potential in Eq. (4.6)

$$\Phi^{(i)}(u,v) = -\frac{Z_0 I_0}{\pi} \sum_{n=1}^{\infty} \left[\frac{\cosh nu \cos nv \cosh nu_1 \cos nv_1}{\cosh nu_0} + \frac{\sinh nu \sin nv \sinh nu_1 \sin nv_1}{\sinh nu_0} \right] e^{-nu_0}. \tag{4.35}$$

This potential can be expressed in terms of x and y by using Eq. (4.12). Specifically we find

$$\Phi^{(i)}(x,y) = -\frac{Z_0 I_0}{\pi} \sum_{n=1}^{\infty} e^{-nu_0} \left[\frac{\mathrm{Re}T_n(\frac{x+iy}{c})\mathrm{Re}T_n(\frac{x_1+iy_1}{c})}{\cosh nu_0} + \frac{\mathrm{Im}T_n(\frac{x+iy}{c})\mathrm{Im}T_n(\frac{x_1+iy_1}{c})}{\sinh nu_0} \right]. \tag{4.36}$$

It is now a simple matter to calculate the parameters associated with the coherent and incoherent tunes. These come, respectively, from the xx_1 and yy_1 terms in the expansion of the potential for small x, x_1, y, y_1 and from the $x^2 - y^2$ terms in the potential for $x_1 = 0, y_1 = 0$. Using

$$T_n(\cos \theta) = \cos n\theta \ , \quad T_n(\sin \phi) = \cos n(\pi/2 - \phi), \tag{4.37}$$

we can write, for $\phi \ll 1$,

$$T_n(\sin \phi) \cong \cos \frac{n\pi}{2} \left[1 - \frac{n^2 \phi^2}{2} \right] + n\phi \sin \frac{n\pi}{2}, \tag{4.38}$$

and therefore, to order z^2

$$T_n(z) \cong \left[1 - \frac{n^2 z^2}{2} \right] \cos \frac{n\pi}{2} + nz \sin \frac{n\pi}{2}. \tag{4.39}$$

The "coherent" part of the potential then becomes

$$\Phi_{\mathrm{coh}}^{(i)}(x,y) = -\frac{Z_0 I_0}{\pi} \left[\frac{xx_1}{c^2} \sum_{\substack{n=1 \\ \mathrm{odd}}}^{\infty} \frac{n^2 e^{-nu_0}}{\cosh nu_0} + \frac{yy_1}{c^2} \sum_{\substack{n=1 \\ \mathrm{odd}}}^{\infty} \frac{n^2 e^{-nu_0}}{\sinh nu_0} \right]. \tag{4.40}$$

Similarly, the "incoherent" part of the potential can be written as

$$\Phi_{\mathrm{incoh}}^{(i)}(x,y) = \frac{Z_0 I_0}{2\pi} \frac{(x^2 - y^2)}{c^2} \left[\sum_{\substack{n=2 \\ \mathrm{even}}}^{\infty} \frac{n^2 e^{-nu_0}}{\cosh nu_0} \right]. \tag{4.41}$$

V. BEAM PIPE OF RECTANGULAR CROSS SECTION

A. Green function

The Poisson equation is written in Eq. (4.1) for a rectangular beam pipe whose boundaries are at $x = \pm a$, $y = \pm b$. If we expand $\Phi(x,y)$ into a Fourier series in the y coordinate

$$\Phi(x,y) = \sum_{n=1}^{\infty} F_n(x) \sin \frac{n\pi}{2b}(y + b), \tag{5.1}$$

with the boundary conditions $F_n(-a) = F_n(a) = 0$, we can easily show that $F_n(x)$ must satisfy

$$\frac{d^2 F_n}{dx^2} - \left(\frac{n\pi}{2b} \right)^2 F_n = -\frac{Z_0 I_0}{b} \sin \frac{n\pi}{2b}(b + y_1)\delta(x - x_1). \tag{5.2}$$

Clearly $F_n(x)$ is a one-dimensional Green function which can be written as

$$F_n(x) = \frac{2Z_0 I_0}{n\pi} \frac{\sin \frac{n\pi}{2b}(b+y_1)}{\sinh \frac{n\pi a}{b}} \begin{cases} \sinh \frac{n\pi}{2b}(x+a) \sinh \frac{n\pi}{2b}(a-x_1) , & x < x_1 \\ \sinh \frac{n\pi}{2b}(a+x_1) \sinh \frac{n\pi}{2b}(a-x) , & x > x_1. \end{cases} \tag{5.3}$$

The two-dimensional Green function is therefore

$$\Phi(x,y) = \frac{2Z_0 I_0}{\pi} \sum_{n=1}^{\infty} \frac{\sin \frac{n\pi}{2b}(y+b) \sinh \frac{n\pi}{2b}(b+y_1)}{n \sinh \frac{n\pi a}{b}} \begin{cases} \sinh \frac{n\pi}{2b}(x+a) \sinh \frac{n\pi}{2b}(a-x_1) , & x < x_1 \\ \sinh \frac{n\pi}{2b}(a+x_1) \sinh \frac{n\pi}{2b}(a-x) , & x > x_1. \end{cases} \tag{5.4}$$

The form in Eq. (5.4) converges exponentially as long as $|x - x_1|/b$ is not too small. An alternate form which converges as long as $|y - y_1|/a$ is not too small is obtained by interchanging a and b, x and y, x_1 and y_1 in Eq. (5.4).

B. Image potential

For the rectangular beam pipe, a two-step process is used to remove the self-potential from Eq. (5.4). The first step is to take the limit as $a \to \infty$ in Eq. (5.4). Specifically, we find

$$\Phi^{a\to\infty}(x,y) = \frac{Z_0 I_0}{2\pi} \sum_{n=1}^{\infty} e^{-\frac{n\pi}{2b}|x-x_1|} \left[\frac{\cos \frac{n\pi}{2b}(y-y_1) - \cos \frac{n\pi}{2b}(2b+y+y_1)}{n} \right]. \tag{5.5}$$

Since

$$\sum_{n=1}^{\infty} \frac{\cos n\sigma e^{-n\lambda}}{n} = -\frac{1}{2}\ln(1 - 2e^{-\lambda}\cos\sigma + e^{-2\lambda}) \tag{5.6}$$

(obtained by taking $d/d\lambda$ and summing the resulting geometric series), we can write

$$\Phi^{a\to\infty}(x,y) = \frac{Z_0 I_0}{4\pi}\ln \left\{ \frac{\sinh^2 \frac{\pi(x-x_1)}{4b} + \cos^2 \frac{\pi(y-y_1)}{4b}}{\sinh^2 \frac{\pi(x-x_1)}{4b} + \sin^2 \frac{\pi(y-y_1)}{4b}} \right\}. \tag{5.7}$$

We can now take the limit $b \to \infty$ in Eq. (5.7) to obtain

$$\Phi^{a,b\to\infty}(x,y) = -\frac{Z_0 I_0}{4\pi}\ln \left[\frac{(x-x_1)^2 + (y-y_1)^2}{(4b/\pi)^2} \right], \tag{5.8}$$

which gives the correct $-(Z_0 I_0/2\pi)\ln r$ dependence on the distance between (x,y) and (x_1, y_1). We now construct the image field

$$\Phi^{image}(x,y) = \Phi(x,y) - \Phi^{a\to\infty}(x,y) + \Phi^{a\to\infty}(x,y) - \Phi^{a,b\to\infty}(x,y). \tag{5.9}$$

From Eqs. (5.4) and (5.5) we then find

$$\Phi(x,y) - \Phi^{a\to\infty}(x,y) = -\frac{Z_0 I_0}{\pi} \sum_{n=1}^{\infty} \frac{\sin \frac{n\pi}{2b}(y+b) \sin \frac{n\pi}{2b}(b+y_1)}{n} e^{-\frac{n\pi a}{2b}} \left[\frac{\sinh \frac{n\pi x}{2b} \sinh \frac{n\pi x_1}{2b}}{\sinh \frac{n\pi a}{2b}} + \frac{\cosh \frac{n\pi x}{2b} \cosh \frac{n\pi x_1}{2b}}{\cosh \frac{n\pi a}{2b}} \right],$$

and from Eqs. (5.7) and (5.9) we find

$$\text{(5.10)}$$

$$\Phi^{a\to\infty}(x,y) - \Phi^{a,b\to\infty}(x,y) = \frac{Z_0 I_0}{4\pi}\ln \Bigg\{ \left[\sinh^2 \frac{\pi}{4b}(x-x_1) + \cos^2 \frac{\pi}{4b}(y-y_1) \right] \left(\frac{\pi}{4b} \right)^2$$

$$\times \left[\frac{(x-x_1)^2 + (y-y_1)^2}{\sinh^2 \frac{\pi}{4b}(x-x_1) + \sin^2 \frac{\pi}{4b}(y-y_1)} \right] \Bigg\}. \tag{5.11}$$

The image potential is therefore the sum of Eqs. (5.10) and (5.11). Note that Eq. (5.10) converges as $\exp(-n\pi a/b)$ for large n, and that the term in the second set of square brackets in Eq. (5.11) is well behaved at $x = x_1, y = y_1$.

Once again, the parameters associated with the coherent and incoherent tunes can be obtained by extracting the xx_1, yy_1, and $(x^2 - y^2)$ terms in an expansion in powers of x, x_1, y, y_1. After considerable algebra, the results

can be written as

$$\Phi^{(i)}_{coh}(x,y) = -\frac{Z_0 I_0}{4b^2} \left\{ xx_1 \left[\frac{1}{12} + \sum_{\substack{n=1 \\ odd}}^{\infty} \frac{ne^{-\frac{n\pi a}{2b}}}{\sinh \frac{n\pi a}{2b}} \right] \right.$$

$$\left. + yy_1 \left[\frac{1}{6} + \sum_{\substack{n=1 \\ even}}^{\infty} \frac{ne^{-\frac{n\pi a}{2b}}}{\cosh \frac{n\pi a}{2b}} \right] \right\} \tag{5.12}$$

and

$$\Phi^{(i)}_{\text{incoh}}(x,y) = \frac{Z_0 I_0 \pi}{8b^2}(x^2 - y^2)\left[\frac{1}{12} - \sum_{\substack{n=1 \\ \text{odd}}}^{\infty}\frac{ne^{-\frac{n\pi a}{2b}}}{\cosh\frac{n\pi a}{2b}}\right].$$

(5.13)

Clearly Eqs. (5.12) and (5.13) are equally well presented by simultaneously interchanging x and y, x_1 and y_1, and a and b. From this, it is easy to verify that $\Phi^i_{\text{incoh}}(x,y) = 0$ for $a = b$, as it must be from symmetry arguments.

VI. COUPLING IMPEDANCES

It is now a simple matter to obtain the longitudinal and transverse coupling impedances by evaluating the line integrals in Eqs. (2.9) and (3.1) using explicit expressions for the fields on the boundary obtained for the elliptical beam pipe using Eqs. (4.17) and (4.21)–(4.24), and for the rectangular beam pipe using Eq. (5.4).

A. Elliptical beam pipe

For the longitudinal impedance we use Eq. (4.17) for $x_1 = 0, y_1 = 0$ in the form

$$|H_{1s}|^2 = \frac{|E_u|^2}{Z_0^2} = \frac{|I_0|^2}{4\pi^2}\frac{Q_0^2(v)}{h^2(v)}.$$

(6.1)

Since the metric is $ds = hdv$, Eq. (2.9) gives

$$\frac{Z_\parallel(k)}{Z_0} = \frac{kL\delta(1+j)}{8\pi^2}\int_0^{2\pi}\frac{dvQ_0^2(v)}{h(v)}.$$

(6.2)

Using the harmonic number $n_h = kL/2\pi$, we obtain

$$\frac{Z_\parallel(k)}{n_h Z_0} = \frac{(1+j)\delta}{2b}G_0(u_0),$$

(6.3)

where [7]

$$G_0(u_0) = \frac{\sinh u_0}{2\pi}\int_0^{2\pi}\frac{Q_0^2(v)dv}{[\sinh^2 u_0 + \sin^2 v]^{1/2}}$$

(6.4)

and where $Q_0(v)$ is defined in Eqs. (4.22) and (4.25). Here $G_0(u_0)$ is normalized so that $G_0(\infty) = 1$, reproducing the known result for a circular beam pipe in Eq. (6.4).

For the transverse impedance, the drive current in Eq. (3.1) requires us to use $2x_1 Q_{1x}(v)/c$ in place of Q_0 in the expression for $|H_{1s}|^2$ in Eq. (3.7). In this way we obtain

$$\frac{Z_{1x}(k)}{Z_0} = \frac{L(1+j)\delta}{2\pi b^3}G_{1x}(u_0),$$

(6.5)

where [7]

$$G_{1x}(u_0) = \frac{\sinh^3 u_0}{4\pi}\int_0^{2\pi}\frac{Q_{1x}^2(v)dv}{[\sinh^2 u_0 + \sin^2 v]^{1/2}},$$

(6.6)

and where $Q_{1x}(v)$ is defined in Eqs. (4.23) and (4.26). Once again, the normalization of $G_{1x}(u_0)$ is chosen so that $G_{1x}(\infty) = 1$, reproducing the known result for a

circular beam pipe in Eq. (6.6). The corresponding expressions for $Z_{1y}(k)$ and $G_{1y}(u_0)$ are obtained by using $Q_{1y}(v)$ instead of $Q_{1x}(v)$.

B. Rectangular beam pipe

Our first step is to obtain $E_{1x} = Z_0 H_{1g}$ on the wall $x = a$ by expanding $-\partial\Phi/\partial x$ in Eq. (5.4) up to terms linear in x_1 and y_1. In this way we find

$$H_{1y}(a,y) = \frac{I_0}{2b}[P_0(y) + x_1 P_{1x}(y) + y_1 P_{1y}(y)],$$

(6.7)

where

$$P_0(y) = \sum_{\substack{n=1 \\ \text{odd}}}^{\infty}\frac{\cos(n\pi y/2b)}{\cosh(n\pi a/2b)},$$

(6.8)

$$P_{1x}(y) = \frac{\pi}{2}\sum_{\substack{n=1 \\ \text{odd}}}^{\infty}\frac{n\cos(n\pi y/2b)}{\sinh(n\pi a/2b)},$$

(6.9)

$$P_{1y}(y) = \frac{\pi}{2}\sum_{\substack{n=2 \\ \text{even}}}^{\infty}\frac{n\sinh(n\pi y/2b)}{\cosh(n\pi a/2b)}.$$

(6.10)

For the longitudinal impedance we take $x_1 = 0, y_1 = 0$ and integrate $P_0^2(y)$ over y from $-b$ to b. The contribution from $x = -a$ doubles the result. In this way we obtain for the longitudinal impedance

$$\frac{Z_\parallel(k)}{n_h Z_0} = \frac{(1+j)\delta}{2b}F_0\left(\frac{b}{a}\right),$$

(6.11)

where

$$F_0(\lambda) = \pi\left[\sum_{\substack{n=1 \\ \text{odd}}}^{\infty}\frac{1}{\cosh^2(n\pi/2\lambda)} + \lambda\sum_{\substack{n=1 \\ \text{odd}}}^{\infty}\frac{1}{\cosh^2(n\pi\lambda/2)}\right].$$

(6.12)

Here we have included the contribution on the walls $y = \pm b$ by interchanging a and b. In an analogous manner, we find that $Z_{1x}(k)$ is related to the integral of $P_{1x}^2(y)$ over y and the corresponding contribution from the walls at $y = \pm b$. After considerable algebra, we find

$$\frac{Z_{1x}(k)}{Z_0} = \frac{L(1+j)\delta}{2\pi b^3}F_{1x}\left(\frac{b}{a}\right),$$

(6.13)

where

$$F_{1x}(\lambda) = \frac{\pi^3}{8}\left[\sum_{\substack{n=1 \\ \text{odd}}}^{\infty}\frac{n^2}{\sinh^2(n\pi/2\lambda)} + \lambda^3\sum_{\substack{n=2 \\ \text{even}}}^{\infty}\frac{n^2}{\cosh^2(n\pi\lambda/2)}\right].$$

(6.14)

The transverse impedance in the y direction is then ob-

tained by exchanging x for y in Eqs. (6.13) and (6.14), and by moving the factor λ^3 to the first sum in the brackets in Eq. (6.14).

Equations (6.12) and (6.16) are in a form which permits taking the limit $a/b \to \infty$, converting the sums involving $(n\pi b/2a)$ to integrals. In fact, using

$$\int_0^\infty \frac{dz}{\cosh^2 z} = 1,$$

$$\int_0^\infty \frac{z^2 dz}{\cosh^2 z} = \frac{\pi^2}{12},$$

$$\int_0^\infty \frac{z^2 dz}{\sinh^2 z} = \frac{\pi^2}{6},$$

(6.15)

one finds, for $a/b \to \infty$, that

$$F_0(0) = 1, \quad F_{1x}(0) = \pi^2/24, \quad F_{1y}(0) = \pi^2/12 \qquad (6.16)$$

correspond to the appropriate values for parallel plates.

A graph of the numerical values of G_0, G_{1x}, and G_{1y} for the elliptical pipe is presented in Fig. 1 as a function of the "nome" $q = (a - b)/(a + b)$. The values for $q = 1$ correspond to parallel plates and are seen to agree with the corresponding values for the $a/b \to \infty$ limit for the rectangular case in Eq. (6.16). The graph of the numerical values of F_0, F_{1x}, F_{1y} for the rectangular case is presented in Fig. 2 as a function of $q = (1 - \lambda)/(1 + \lambda) = (a - b)/(a + b)$. The similarity between the two figures is striking, but perhaps not surprising, since the ellipticity of the ellipse and rectangle are very similar.

The longitudinal and transverse resistive wall impedances have also been analyzed by Neil and Sessler [8] and by Laslett, Neil, and Sessler [9], respectively, not including losses on the side walls ($x = \pm a$). Their results are given in terms of the scaled impedance parameter V, and in the limit $\gamma \to \infty$ their expressions are in agree-

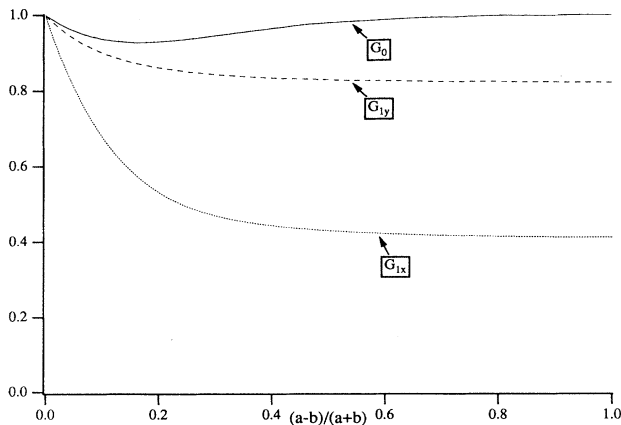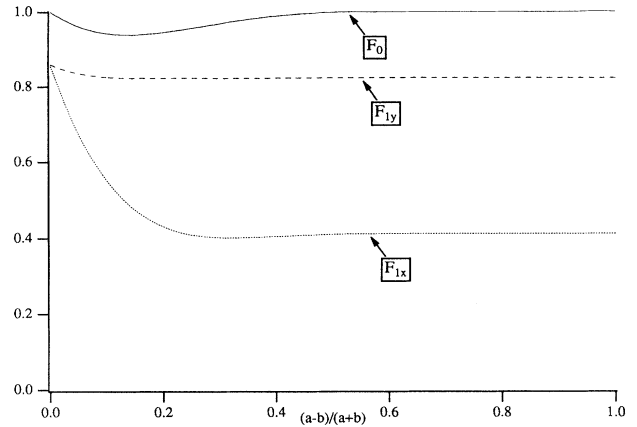FIG. 2. Numerical values of $F_0(q), F_{1x}(q)$, and $F_{1y}(q)$ for the rectangular case as a function of $q = (1 - \lambda)/(1 + \lambda) = (a - b)/(a + b)$.

ment with the parts of Eqs. (6.12) and (6.14) which correspond to the surfaces $y = \pm b$.

VII. COUPLING IMPEDANCE OF HOLES IN THE BEAM PIPE

For completeness we include a brief discussion of the results for the coupling impedance of a small hole in a beam pipe [10]. We start with Eqs. (2.7) and (3.6) and assume that the dimensions of the hole are small compared with the wavelength. In this case, the coupling integral

$$L \oint ds E_z H_{1s}^* = \int dS \, \mathbf{n} \cdot \mathbf{E} \times \mathbf{H}_1, \qquad (7.1)$$

written here as an integral over the interior aperture of the hole, can be expressed in terms of the inside electric polarizability, χ_{in}, and inside magnetic susceptibility, ψ_{in}, of the hole as

$$\int dS \, \mathbf{n} \cdot \mathbf{E} \times \mathbf{H}_1 = -j \frac{k|H_{1s}|^2}{2} (\psi_{in} - \chi_{in}). \qquad (7.2)$$

We have here assumed that the field outside the beam pipe can be ignored. A more complete discussion of the inside and outside polarizability and susceptibility is given elsewhere [11], including numerical results for a circular hole in a wall of finite thickness.

Once ψ_{in} and χ_{in} are known, the impedance can be calculated from $|H_{1s}|^2$ along the beam pipe wall. For the longitudinal coupling impedance, this quantity is proportional to $Q_0^2(v)$ in Eq. (4.2) for an elliptical beam pipe, where v is the azimuthal coordinate of the hole, and to $P_0^2(y)$ [or $P_0^2(x)$] in Eq. (6.8) where x, y are the coordinates of the hole. For the transverse coupling impedance, the corresponding quantities are $Q_{1x,y}^2(v), P_{1x}^2(x, y), P_{1y}^2(x, y)$, given in Eqs. (4.23), (4.24) and (6.9), (6.10).

The impedances of well separated holes (by at least a

FIG. 1. Numerical values of $G_0(q), G_{1x}(q)$, and $G_{1y}(q)$ for the elliptical pipe as a function of the "nome" $q = (a - b)/(a + b)$.

few hole diameters) can be added to each other, since the surface integral in Eq. (7.1) extends over all holes.

VIII. SUMMARY

General expressions have been obtained for the longitudinal and transverse coupling impedances of a beam pipe in the ultrarelativistic limit in terms of integrals of the fields over a surface (usually the beam pipe) which surrounds the beam. For a resistive wall these expressions can be written in terms of integrals of the square of the tangential magnetic field over the surface of the beam pipe. The magnetic field can itself be obtained from the solution of the Poisson equation in the two transverse coordinates for a monopole singularity (longitudinal impedance) and for a dipole singularity (transverse impedance).

Detailed expressions are given for an elliptical beam pipe and for a rectangular beam pipe, including the image fields which are useful for determining the coherent and incoherent tune shifts. The expressions involve well-convergent series and are well suited to numerical computation. Such numerical results are provided as a function of $(a - b)/(a + b)$ where $2a$ and $2b$ are the major and minor axes of the ellipse or the width and height of the rectangle. The results for the ellipse agree with the well-known results for a circle when $a = b$, and the results for both cases agree with the results for parallel plates in the limit $a \to \infty$.

It may be useful to reiterate at this point that we have assumed that $\gamma \to \infty$ in our calculation of impedance. In fact, our calculation is greatly simplified in this limit, particularly for the case of the elliptical pipe. However, for large but finite γ, the impedance results will depart from those given in Eq. (6.3), (6.5), (6.11), and (6.13) at frequencies for which $kb \gtrsim \gamma$ where b is a characteristic dimension of the chamber cross section. We note that results for finite γ for a chamber of circular and rectangular cross section have been available [8, 9] for some time.

In addition, our treatment of wall losses uses the reasonable assumption that the skin depth is small compared to the characteristic dimension of the chamber cross section. For the unlikely situation where $\delta \gtrsim b$, the analysis is much more complicated and unlikely to be analytically tractable, except for a chamber of circular cross section.

[1] R.L. Gluckstern, J.B.J. van Zeijts, and B. Zotter, CERN Report No. SL/AP 92-18, April 1992 (unpublished).

[2] R.L. Gluckstern and F. Neri, IEEE Trans. Nucl. Sci. NS-32, 2403 (1985).

[3] O. Napoly, Saclay Report No. CEA, DPhN/STAS/91-R12 (1991) (unpublished).

[4] Further details can be found in P. M. Morse and H. Feshbach, Methods of Theoretical Physics (McGraw-Hill, New York, 1953), pp. 1202ff.

[5] See, e.g., Handbook of Mathematical Functions, edited by M. Abramowitz and I. Stegun (Dover, New York, 1965), Eqs. 16.23.4-6.

[6] L. Palumbo and V.G. Vaccaro, Nuovo Cimento A 89 (1985).

[7] The notation for $G(u_0)$ is slightly different from that in Ref. [1] in order to give a more useful form for an ellipse with large eccentricity.

[8] V.K. Neil and A.M. Sessler, Rev. Sci. Instrum. 36, 429 (1965).

[9] L.J. Laslett, V.K. Neil, and A.M. Sessler, Rev. Sci. Instrum. 36, 436 (1965).

[10] For greater detail, see R.L. Gluckstern, Phys. Rev. A 46, 1106 (1992); 46, 1110 (1992).

[11] R.L. Gluckstern and J.A. Diamond, IEEE Trans. Microwave Theory Tech. 39, 274 (1991).